

Original Article

# Utilization of D-3-hydroxybutyrate by the isolated perfused heart under global no-flow ischemia and stress conditions

Abdurazzaq M. N. Sultan

Umm Al Qura University- Faculty of Medicine, Department of Biochemistry.

**Correspondence :**

**Prof. Abdurazzaq M. N. Sultan**

Department of Biochemistry,

Faculty of Medicine,

Umm Al-Qura University,

Makkah 21955,

Saudi Arabia.

asultan@uqu.edu.sa

Tel: +96625270064

Fax: +96625282385

Mobile: 00966505561986

## إستخدام الموجات الصوتية في تشخيص خشونة مفصل الركبة الروماتيزمي

أ.د. عبد الرزاق بن محمد نور سلطان  
قسم الكيمياء الحيوية ,كلية الطب جامعة أم القرى  
asultan@uqu.edu.sa

### الملخص العربي

في الظروف الاعتيادية يفضل القلب استخدام هيدروكسي بيوتريت عن الجلوكوز أو الاحماض الدهنية كمصدر للطاقة . يثبط هيدروكسي بيوتريت أكسدة الجلوكوز والأحماض الدهنية بينما الاجهاد الفسيولوجي وغير الفسيولوجي ينشط أكسدة الجلوكوز والأحماض الدهنية. الدراسة التالية تبحث في تأثير الإجهاد الكيميائي وغياب سريان الشريان التاجي على أكسدة هيدروكسي بيوتريت وإنتاج أسيتوأسيتيت في وجود وغياب محفزات ومثبطات مسارات الاشارات البيو كيميائية.

التأثير المحفز لمركب داينتروفينول على استهلاك هيدروكسي بيوتريت في القلب يتناسب طردي مع تركيز المحفز. غياب سريان الشريان التاجي وأينومايسين منشط CaMKK وأنيسومايسين منشط P38MAPK تحفز استهلاك هيدروكسي بيوتريت في القلب , المركبين STO-609 و PD-169316 يبطلان التأثير التحفيزي السابق.

### الاستنتاج:

داينتروفينول منشط للمسارين AMPK و P38.MAPK في القلب وأنيسومايسين منشط P38MAPK وأينومايسين منشط CaMKK , جميعهم يحفزون استهلاك أو استخدام بيتاهيدروكسي بيوتريت في القلب, تثبيط المسارات السابقة AMPK و P38.MAPK و CaMKK في القلب يبطل التحفيز الناتج عن تنشيط مسارات AMPK و P38 MAPK في القلب. النتائج تشير إلى امكانية مساهمة AMPK و P38.MAPK أثناء تعرض القلب للإجهاد أو غياب الشريان التاجي في القلب وتنظيم أيض بيتاهيدروكسي بيوتريت وأن التأثير المحفز للاسكيميا على أيض هيدروكسي بيوتريت في القلب يتم عبر مسارات الاشارات البيو كيميائية لكل من AMPK و P38.MAPK

## ABSTRACT

It is known that under normal conditions, D-3-hydroxybutyrate (D-3-HB) utilization is preferred over glucose and fatty acids by the isolated perfused heart. Moreover, D-3-HB inhibits oxidation whereas physiological and non-physiological stressors stimulate the oxidation of both major energy substrates. The following study investigates the effect of chemical stress and global no-flow ischemia-reperfusion on the utilization of D-3-HB and acetoacetate production in the isolated perfused rat heart, in the presence and absence of reported activators and inhibitors of some signaling pathways. The uncoupling of the oxidative phosphorylation of 2, 4-dinitrophenol (DNP) enhanced D-3-HB utilization in a concentration dependent manner. Global non-flow ischemia-reperfusion, and ionomycin and anisomycin, the activators of Ca<sup>2+</sup>-calmodulin-dependent protein kinase kinase (CaMKK) and p38 mitogen-activated protein kinase (p38 MAPK), respectively, stimulate the utilization of D-3-HB. On the other hand, the inhibitors STO-609 and PD-169316 abolish ionomycin, anisomycin and global no-flow ischemia-stimulated utilization of D-3-HB. We conclude that: DNP [an activator of both cardiac AMP-activated protein kinase (AMPK) and p38 MAPK], anisomycin (a selective activator of p38 MAPK), and ionomycin (a CaMKK activator) stimulate D-3-HB utilization in heart, and this stimulation is either partially or completely abolished by selective inhibitors of the above mentioned kinases. Our findings suggest the possible involvement of AMPK and p38 MAPK during stress in regulating D-3-HB utilization, and that the ischemia-reperfusion stimulatory effect may possibly be mediated by the AMPK and p38 MAPK signaling pathways for further investigation.

### Keywords

D-3-HB, Stress, AMPK, CaMKK, p38MAPK, Cardiac metabolism

## INTRODUCTION

The heart primarily utilizes fatty acids, glucose and, ketone bodies as a sources of energy (1,2). Ketone bodies compete with glucose and fatty acids for utilization by the heart (3, 4, 5). D-3-hydroxybutyrate (D-3-HB) is not only an energy substrate but also plays a regulatory role in cardiac metabolism: it improves metabolic efficiency, decreases free radical damage, and presents cardioprotective effects (6). Fasting enhanced and chronic diabetes decreased D-3-hydroxybutyrate utilization in the isolated perfused rat heart (7, 8).

During exposure to such stressors as ischemia, ischemia-reperfusion, hypoxia, and anoxia, the activation of the AMP-activated protein kinase (AMPK) signaling pathway plays a significant role in controlling cardiac metabolism. The stimulation of AMPK activity enhances catabolic pathways to provide the heart with ATP, and inhibits the consumption of ATP since maintaining cellular ATP levels is vital for heart viability and function under stress related conditions (9, 10). The regulation of fatty acids and glucose metabolism in heart is mediated by the AMPK signaling pathway during physiological and non-physiological stress. Heart AMPK activation increases

glucose and fatty acid oxidation and inhibits protein synthesis (9,11, 12, 13, 14).

To the best of our knowledge, there has been no publications in the literature on the effect of ischemia and chemical stress on the utilization of D-3-hydroxybutyrate, and the role of the AMPK and p38 mitogen-activated protein kinase (p38 MAPK) signaling pathways in the regulation of D-3-hydroxybutyrate. The purpose of this investigation was to study D-3-hydroxybutyrate utilization under chemical stress and global no-flow ischemia, in the isolated perfused rat heart in the presence and absence of reported activators and inhibitors of some signaling pathways. We used DNP as a chemical stressor to mimic hypoxia and to induce an energy demand in the heart. We also used ischemia-reperfusion to investigate the effect of metabolic stress on the utilization of D-3-hydroxybutyrate

## MATERIAL AND METHODS

### Animals

Normal male Albino Wister rats weighing between 250-350 g were used in the present study. Animals were housed under a constant room temperature of 22° C and a controlled light cycle (lights on between 06.00-18.00 h). The rats were fed ad libitum and had free access to food and water. The diet consisted of pellets containing 13% protein and 3% fat, manufactured by Grains and Flour Mills Organization, Jeddah, Saudi Arabia. All experiments were conducted in accordance with the guidelines of Umm Al-Qura University Council of Animal Care and were approved by the animal care committee of Umm Al-Qura Research Institute.

### Chemicals

DL-3-hydroxybutyrate (sodium salt) (DL-3-HB), nicotinamide adenine dinucleotide

(disodium salt, oxidized and reduced forms), D-3-hydroxybutyrate dehydrogenase (EC.1.1.1.30), acetoacetate (lithium salt)(Ac), 2,4-dinitrophenol (DNP), Adenine 9-β-D-arabinofuranoside (Ara-A), 5-Iodotubercidin(Itub), 7-Oxo- 7-H-benzimidazo [2.1-] benz[de] isoquinoline-3-carboxylic acid - acetic acid (STO-609), Ionomycin(Iono), Pinacidil, PD-169316(PD), Anisomycin (Aniso), and Dimethylsulfoxid(DMSO) as vehicle (v), and all other chemicals maintained the highest available quality and were obtained from SIGM-ALDRICH, USA

### Media

The saline medium consisted of 142.2 mM sodium chloride and 0.5 mM sodium bicarbonate, and when equilibrated with atmospheric CO<sub>2</sub> at 4°C, had a pH of 7.4. The saline medium was used during the preparation of cannulation to cool the heart following excision.

Hearts were perfused for either two hours or 90 min with Krebs-Henseleit medium modified to contain half of the concentration of calcium and magnesium (MKHM), and oxygenated by equilibration with 5% CO<sub>2</sub> in oxygen. DL-3-HB was included at 5 mM corresponding to an initial concentration of the metabolically active D-3-HB of 2.5 mM. When the vehicle (v), dimethylsulfoxide (DMSO) was used, its concentration was no more than 0.2% v:v, and the addition of other substances are shown in the results and in the figure legends.

### Perfusion Method

We utilized the Fisher and O'Brien(15) and Sultan (2) non-working heart perfusion technique to perfuse the rat hearts. This technique involves the continuous infusion of fresh media into a volume of recirculating perfusate that is kept constant by balanced withdrawal. Hearts (158) were removed from

fed rats under light diethyl ether anesthesia and placed in a cooled saline medium at 4°C and prepared for cannulation. Hearts were perfused with MKHM containing substance(s) at a pressure of 40 mmHg, and at an infusion rate of  $30.65 \pm 0.08 \text{ ml.hr}^{-1}$  (158) for 120 or 90 min, and a perfusate temperature of 37°C. The perfusate was passed through a 47 mm Millipore disc of 0.47 µm pore diameter (Millipore Corporation, Bedford, Mass, USA) supported by a Whatman No. 54 paper filter. Samples of perfusate were collected for five minutes, and alternate samples were analyzed. We collected twelve samples during the 2<sup>nd</sup> hour or six samples during the last 30 min of perfusion, respectively. Next, either six or three alternate fractions were used to determine the D-3-HB and Acetoacetate (Ac) concentrations.

Coronary flow of each perfused heart was measured at the 3<sup>rd</sup> minute (57.57±1.33 (118) ml.g.dry w<sup>-1</sup>. min<sup>-1</sup>) and a successful preparation. Hearts with a coronary flow less than 30ml.g. dry w<sup>-1</sup>. min<sup>-1</sup> were suspected of being blocked and were disregarded(2).

#### Global no-flow ischemia protocol

Three groups of hearts were perfused with MKHM, containing DL-3-HB (5mM) in the absence and presence of either PD-169316 (1µM) or STO-609 (2.5µM) for 10 minutes. This served as the equilibration period of aerobic perfusion as coronary flow reached  $60 \pm 1.61 \text{ ml. g.dry wt}^{-1} \cdot \text{min}^{-1}$  followed by 15 minutes of global no-flow ischemia. Then the perfusate flow through the heart was completely interrupted resulting in a subsequent 65 minute period of aerobic reperfusion with MKHM containing DL-3-HB (5mM) in the absence and presence of PD-169316 or STO-609. The coronary flow at the end of the reperfusion period was  $63.71 \pm 2 \text{ ml. g.dry wt}^{-1} \cdot \text{min}^{-1}$ . Heart beats ceased between 2-4 minutes after stopping the flow of the perfusate and restarted after 1-2 minutes of reperfusion. On examining the

heart at the end of perfusion period, the heart was soft, and there were no apparent ischemic patches.

#### Analytical methods

The estimation of D-3-hydroxybutyrate (D-3-HB) and acetoacetate (Ac) were performed by the methods of Williamson and Mellanby (16) and Mellanby and Williamson, respectively.

Calculation and expression of the results

In the steady state condition, the concentrations of the substrate in successive fractions were not measurably different. The second hour of the perfusion period represents the steady state period. During this period, the following equation was used to estimate the rate of D-3-hydroxybutyrate utilization and acetoacetate production:

$$u = \frac{i(x-a)}{w} - \frac{dx}{dt} \quad (1)$$

Where u: the rate of utilization (negative if production), µmoles.g.drywt<sup>-1</sup>.h<sup>-1</sup>

i: the rate of infusion, ml.h<sup>-1</sup>

a: the initial perfusate concentration, mM

x: the perfusate concentration, mM

w: the dry weight of the heart, g

The difference between the rate of D-3-HB utilization and the rate of acetoacetate production is assumed to be the rate of D-3-HB oxidation, and can be calculated.

Results were expressed as a mean of individual experiments ±SEM and the number of observations given in parentheses.

#### **Statistical analysis**

Comparisons between groups were assessed by the two-tailed Student's t-test for independent observations using Texasoft, WINKS SDA Software, 6<sup>th</sup> Edition, Cedar Hill, Texas, 2007.

## RESULTS

### The effect of DNP on D-3-hydroxybutyrate utilization

To establish the effect of DNP on D-3-HB utilization, six groups of hearts were perfused with MKHM containing DL-3-HB (5mM) and different concentrations of DNP. The control group did not contain DNP while the other groups contained DNP at the following concentrations: 5, 10, 25, 50, or 100  $\mu$ M. The rate of D-3-HB utilization and acetoacetate production during the 2nd 60 minutes of perfusion is shown in Figure 1. DNP stimulated D-3-HB utilization by 23%, 34%, and 40% at 10, 25, and 50  $\mu$ M, respectively ( $p \geq 0.001$ ). Regarding the heart rate, no significant effect was observed at 5  $\mu$ M, whereas at 100  $\mu$ M, heart beats were irregular, and the preparation was unstable (four experiments results are not shown). We considered that DNP at 50  $\mu$ M had a maximum effect on D-3-HB utilization without any deterioration of the perfused heart preparation; therefore, all subsequent experiments were performed at this concentration.

**Figure 1.** The effect of dinitrophenol on the rates of D-3-HB utilization and acetoacetate production.

Hearts were perfused with MKHM containing DL-3-HB (5mM) in the absence (control) and presence of dinitrophenol (DNP; 5, 10, 25, or 50  $\mu$ M) for 120 min as described in the methods section. Results indicate means  $\pm$  SEM and the number of individual observations are given in parentheses. The rates of D-3-HB utilization (white bar) and acetoacetate production (black bar), were estimated during the steady state and refer to the last 60 min of

the perfusion period. \* $p \leq 0.001$  DNP vs control.

NB: DL-3-HB (5mM), should be present under every bar but it is as shown in figure for simplicity

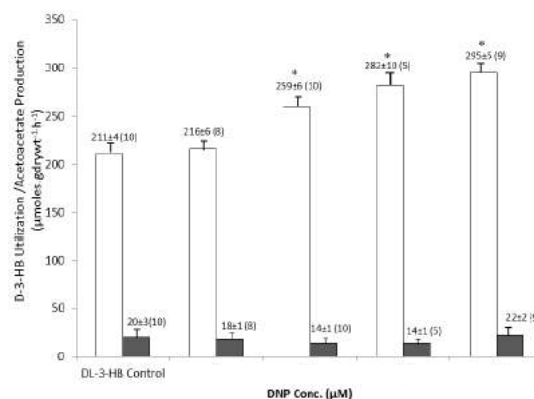


Fig. 1. The effect of dinitrophenol(DNP) on the rates of D-3-HB utilization and acetoacetate production

The stimulatory effect of DNP on the utilization of D-3-HB is concentration dependent, and there is no significant effect of DNP on acetoacetate production. Almost 90-95% of D-3-HB is not recovered as acetoacetate, and it is assumed to be oxidized and provides the heart with energy in the presence and absence of DNP.

### The effect Ara-A and Iodotubercidin

DNP activates AMPK in cardiomyocytes, and Ara-A inhibits DNP-stimulated AMPK phosphorylation and glucose uptake (12). Iodotubercidin (Itub) inhibits adenosine kinase in neonatal hearts (18), basal AMPK $\alpha$ 2 activity in skeletal muscle (19), and decreases AICAR- and cyanide-stimulated glucose uptake in heart papillary muscles (13). We tested the effect of two inhibitors on the action of DNP in stimulating D-3-HB utilization.

Two groups of hearts were perfused with MKHM containing DL-3-HB (5mM)

and vehicle (v) in the presence and absence of DNP (control), and another four groups of hearts were perfused with MKHM containing DL-3-HB, vehicle, and either Ara-A (1mM) or Itub (5 $\mu$ M), in the presence and absence of DNP. Figure 2 shows that both substances Ara-A and Itub inhibited the basal rates of D-3-HB utilization by 26% and 23%  $p \leq 0.005$  and  $p \leq 0.001$ , respectively, and without significant effect on the rate of acetoacetate production in the absence of DNP. Ara-A partially inhibited rates by 8%  $p \leq 0.02$ , and Itub abolished DNP-stimulated D-3-HB utilization without significant effect on acetoacetate production. The vehicle (DMSO) had no significant effect on the utilization of D-3-HB and acetoacetate production in the presence and absence of DNP.

**Figure 2.** The effect of Ara-A and iodotubercidin on the rates of D-3-HB utilization and acetoacetate production in the presence and absence of dinitrophenol.

Hearts were perfused with MKHM containing DL-3-HB (5mM), vehicle (v), and either with or without dinitrophenol (DNP; 50 $\mu$ M) for 90 min as described in the methods section. The addition of either Ara-A (1mM) or iodotubercidin (itub; 5 $\mu$ M) is also shown in the figure. Results indicate means  $\pm$  SEM and the number of individual observations are given in parentheses. The rates of D-3-HB utilization (white bar) and acetoacetate production (black bar), were estimated during the steady state and refer to the last 30 min of the perfusion period.

\* $p \leq 0.005$  Ara-A vs control, \*\* $p \leq 0.001$  Itub vs control, DNP+Itub vs DNP control, \*\*\* $p \leq 0.02$  DNP+Ara-A vs DNP control.

NB: DL-3-HB (5mM) and vehicle (v), should be present under every bar but it is as shown in figure for simplicity

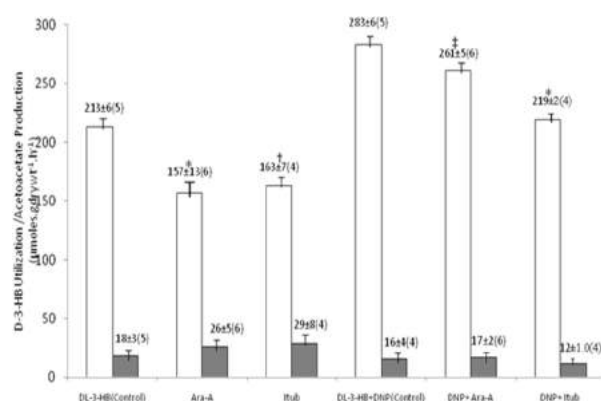


Fig. 2. The effect of Ara-A and iodotubercidin (Itub) on the rates of D-3-HB utilization and acetoacetate production in the presence and absence of dinitrophenol

#### The effect of Ionomycin and STO-609

The calcium ionophore, ionomycin, increased the cytosolic calcium concentration (20) and activated AMPK phosphorylation by the upstream kinase is  $Ca^{2+}$ -calmodulin-dependent protein kinase kinase (CaMKK). This activation was inhibited by STO-609 (21, 22, 23), and DNP also induced an elevation of cytosolic  $Ca^{2+}$  (24, 25, 26). We used ionomycin to activate AMPK through the upstream kinase, CaMKK.

Two groups of hearts were perfused with MKHM containing DL-3-HB (5mM), vehicle, and ionomycin (1.3 $\mu$ M) in the presence and absence of STO-609 (2.5  $\mu$ M). Figure 2 shows ionomycin stimulated the rate of D-3-HB utilization by 28%  $p \leq 0.001$ , and almost all of the utilized D-3-HB was fully oxidized. STO-609 abrogated the ionomycin-stimulated D-3-HB utilization and increased the rate of acetoacetate production to about 9% of the of the utilized D-3-HB  $p \leq 0.005$ . Another two groups of hearts were perfused with MKHM containing DL-3-HB, vehicle, and DNP in the presence and absence of STO-609. Figure 3 shows that STO-609

partially inhibits DNP-stimulated D-3-HB utilization by 16%  $p \leq 0.001$ , and the production of acetoacetate is increased to about 21%  $p \leq 0.001$  of the utilized D-3-HB. In hearts perfused with MKHM containing DL-3-HB, vehicle, and STO-609, STO-609 had no effect on both the basal rate of D-3-HB utilization and on acetoacetate production.

**Figure 3.** The effect of ionomycin, STO-609, and pinacidil on the rates of D-3-HB utilization and acetoacetate production.

Hearts were perfused with MKHM containing DL-3-HB (5mM) and vehicle (v) for 90 min as described in the methods section, with the addition of ionomycin (iono; 1.3  $\mu\text{M}$ ), STO-609 (2.5  $\mu\text{M}$ ), pinacidil (100  $\mu\text{M}$ ) or dinitrophenol (DNP; 50  $\mu\text{M}$ ) to the perfusate as also shown in the figure. Results indicate means  $\pm$  SEM and the number of individual observations are given in parentheses. The rates of D-3-HB utilization (white bar) and acetoacetate production (black bar) were estimated during the steady state and refer to the last 30 min of the perfusion period. \* $p \leq 0.001$  Ionovs control, Ionovs Iono+STO-609, for D-3-HB utilization, and DNP+STO-609 vs DNP control, for Ac production. \*\* $p \leq 0.005$  Ionovs Iono+STO-609 for Ac production.

NB: DL-3-HB (5mM) and vehicle (v), should be present under every bar but it is as shown in figure for simplicity

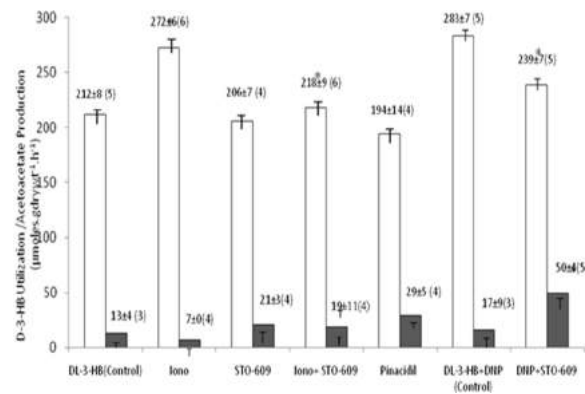


Fig. 3. The effect of ionomycin (Iono) STO-609 and pinacidil on the rates of D-3-HB utilization and acetoacetate production

#### The effect of Pinacidil

Pinacidil is a  $K_{ATP}$  opener, and DNP can acts as  $K_{ATP}$  opener (27, 28). Pinacidil and DNP activate sarcolemmal  $K_{ATP}$  channels in cardiomyocytes (29). AMPK mediates preconditioning in cardiomyocytes by regulating sarcolemmal ATP-sensitive  $K^+$  channels (30). We used pinacidil to investigate whether  $K_{ATP}$  channels could be involved in mediating the effects of DNP.

A group of hearts was perfused with MKHM containing DL-3-HB, vehicle, and Pinacidil(100  $\mu\text{M}$ ). Figure 3 shows that pinacidil had no effect on the basal rate of D-3-HB utilization.

#### The effect of Anisomycin and PD-169316

Anisomycin activates cardiac p38 MAPK in a time- and dose-dependent manner without affecting AMPK (31), and PD-169316 is a selective inhibitor of p38 MAPK (12, 32). DNP stimulates p38 MAPK activity, and PD-169316 inhibits this effect in cardiomyocytes (12). We used anisomycin to activate p38 MAPK, which mimics the ischemia-reperfusion condition(44,45,46).

Two groups of hearts were perfused with MKHM containing DL-3-HB, vehicle, and anisomycin (10 $\mu\text{M}$ ) in the presence and

absence of PD-169316 (1 $\mu$ M). Figure 4 shows that anisomycin stimulated the rate of D-3-HB utilization by 26%  $p \leq 0.001$ , and PD-169316 fully abolished anisomycin-stimulated D-3-HB utilization. Another two groups of hearts were perfused with MKHM containing DL-3-HB, vehicle, and DNP in the presence and absence of PD-169316. Figure 4 shows that PD-169316 statistically had no significant effect on DNP-stimulated D-3-HB utilization. In hearts that were perfused with MKHM containing DL-3-HB, vehicle, and PD-169316, PD-169316 had no effect on the basal rate of D-3-HB utilization. Each of these groups presented acetoacetate production percentage rates at around 8% of the utilized D-3-HB.

**Figure 4.** The effect of anisomycin, PD-169316, and global ischemia-reperfusion on the rates of D-3-HB utilization and acetoacetate production.

Hearts were perfused with MKHM containing DL-3-HB (5mM) and vehicle (v), as described in the methods section, with the addition of anisomycin (aniso; 10  $\mu$ M), PD-169316 (PD; 1  $\mu$ M), or dinitrophenol (DNP; 50  $\mu$ M) to the perfusate as also shown in the figure. Global ischemia-reperfusion was induced as described in the methods section. Results indicate means  $\pm$  SEM and the number of individual observations are given in parentheses. The rates of D-3-HB utilization (white bar) and acetoacetate production (black bar) were estimated during the steady state and refer to the last 30 min of the perfusion period. \*  $p \leq 0.001$  Anisovs control, Anisovs Aniso+PD, ischemia vs ischemia +PD, Ischemiavs Ischemia+STO-609. \*\*  $p \leq 0.002$  Ischemia vs control.

NB: DL-3-HB (5mM) and vehicle (v), should be present under every bar but it is as shown in figure for simplicity

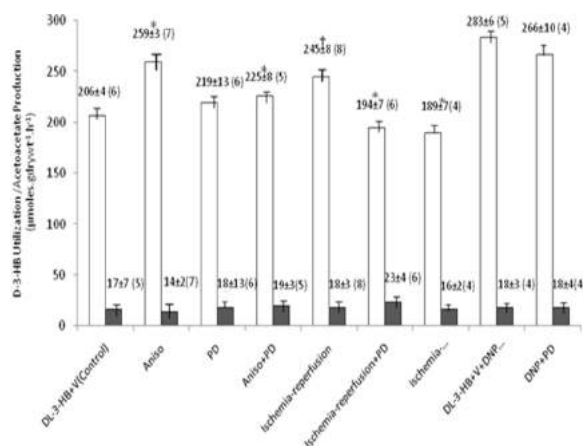


Fig. 4. The effect of anisomycin (Aniso), PD-169316, STO-609 and global ischemia reperfusion on the rates of D-3-HB utilization and acetoacetate production. vehicle (v)

#### The effect of global no-flow ischemia, PD-169316 and STO-609

Hearts were subjected to no-flow ischemia for 15 min and allowed to equilibrate for 10 min, followed by a period of reperfusion for 65 min. The utilization of D-3-HB was estimated during the last 30 min of the reperfusion period. The rate of D-3-HB utilization was increased by 19%  $p \geq 0.001$  during the reperfusion period as shown in Fig. 4. The oxidation rate of D-3-HB was 93% of the utilized D-3-HB. In another two groups of hearts subjected to no-flow ischemia, the addition of either PD169316 (1 $\mu$ M) or STO-609 (2.5 $\mu$ M) to the circulation media abolished the ischemia-reperfusion-stimulated utilization of D-3-HB.

## DISCUSSION

DNP stimulates the utilization of D-3-HB in the isolated perfused heart in a concentration-dependent manner. This stimulatory effect is due to either one or more of the multi effects of DNP. DNP is an uncoupler and causes

mitochondrial membrane depolarization, a reduction in the mitochondrial membrane potential (33, 34), a decrease in myocyte  $\text{NADH}^+$  (26), a raise in the cytosolic concentration of  $\text{Ca}^{2+}$  and increases the AMP/ATP ratio (24, 25, 34). DNP stimulates the activity of AMPK, p38 MAPK and the uptake of glucose in cardiomyocytes (12). Either Ara-A or iodotubercidin decreased the basal rate of D-3-HB utilization, indicating a possible role for AMPK in normal conditions. Ara-A caused partial inhibition of the DNP-stimulated D-3-HB utilization, whereas iodotubercidin abolished the DNP-stimulated D-3-HB utilization indicating the role of AMPK in stressful conditions. The partial inhibition of Ara-A on DNP-stimulated D-3-HB utilization could be due to Ara-A inhibiting the AMPK  $\alpha_2$  isoform (19), which is also predominant in cardiac cells (35, 36). DNP activates both the  $\alpha_1$  and  $\alpha_2$  isoforms of AMPK (37). Therefore, the DNP stimulatory effect could be a result of the activity of the AMPK  $\alpha_1$  isoform. The effect of iodotubercidin could be due to the inhibitory effect on adenosine kinase (18), adenosine transport (38), AMPK  $\alpha_2$  (19) and AMPK $\alpha_1$  (39). Ara-A partially inhibits DNP-stimulated AMPK and glucose uptake in cardiomyocytes (12), and iodotubercidin partially inhibits cyanide-stimulated glucose uptake in heart papillary muscle (13). This is consistent with our findings since Ara-A and Itub inhibit basal D-3-HB utilization.

The inhibition of basal D-3-HB utilization by both Ara-A and Iodotubercidin (selective inhibitors of AMPK $\alpha_2$ ), the partial and complete inhibition of DNP-stimulated D-3-HB utilization by Ara-A and iodotubercidin, respectively, and DNP's ability to raise the cytosolic  $\text{Ca}^{2+}$  concentration and the sensitivity of AMPK $\alpha_2$  to AMP drove researchers to modulate the upstream kinase CaMKK. CaMKK activates AMPK (21, 22,

40), particularly AMPK $\alpha_1$  (41), in response to the rise of cytosolic  $\text{Ca}^{2+}$  independently of the AMP/ATP ratio (42), and DNP increases cytosolic  $\text{Ca}^{2+}$  (24, 25, 26). Ionomycin, a CaMKK activator, stimulated D-3-HB utilization and was then abolished by STO-609, a selective inhibitor of CaMKK (23). This supports the involvement of AMPK in regulating D-3-HB utilization, moreover; it indicates the role of calcium as an intracellular messenger in D-3-HB metabolism. STO-609 partially inhibited DNP-stimulated D-3-HB utilization, indicating that the DNP effect is partially mediated by increasing the level of cytosolic  $\text{Ca}^{2+}$ , further activating CaMKK. These findings support the possibility that the  $\text{Ca}^{2+}$  - CaMKK - AMPK signaling pathway mediates DNP-stimulated D-3-HB utilization.

DNP could also activate  $\text{K}_{\text{ATP}}$  channels by depolarizing the intra-mitochondrial membrane and altering the  $\text{Ca}^{2+}$  cytosolic concentration (27, 28). Pinacidil opens  $\text{K}_{\text{ATP}}$  channels and (29) has no significant effect on the basal rate of D-3-HB utilization, therefore, data do not support that enhancing  $\text{K}_{\text{ATP}}$  channels mediates DNP-stimulated D-3-HB utilization.

The role of p38 MAPK

DNP activates p38 MAPK and AMPK in cardiomyocytes (12), and PD-169316 is a selective inhibitor of cardiac p38 MAPK (32, 12). Anisomycin potently activates cardiac p38 MAPK without stimulating the phosphorylation of AMPK and AKt (31, 43). Anisomycin mimics ischemia-reperfusion in activating p38 MAPK (44, 45, 46). Our finding that anisomycin stimulated D-3-HB utilization and that PD-169316 abolished this stimulation, strongly support the involvement of the p38 MAPK signaling pathway in the regulation of D-3-HB metabolism independent of the AMPK signaling

pathway. We also demonstrated that PD-169316 had no significant effect on both basal D-3-HB utilization and DNP-stimulated D-3-HB utilization; although DNP activated p38 MAPK and PD-169316 partially inhibited p38 MAPK in cardiomyocytes (12). Therefore, we were unable to conclude that the DNP effect on D-3-HB utilization is mediated through the p38 MAPK signaling pathway. However, we did not exclude the involvement of p38 MAPK in D-3-HB regulation since anisomycin-activated D-3-HB utilization is abolished by PD-169316.

In this study, we demonstrated that modulating either the AMPK or p38 MAPK signaling pathways affects D-3-HB utilization. The stimulation and inhibition of the AMPK/p38 MAPK signaling pathways were associated with the stimulation and inhibition of D-3-HB utilization, respectively.

Mimicking either chemical hypoxia or ischemia-reperfusion is associated with the enhancement of the utilization of D-3-HB in the heart. Ischemia activates AMPK and p38 MAPK, and the activation of p38 MAPK occurs independently of AMPK (47). PD-169316, an inhibitor of p38 MAPK, and STO-609, an inhibitor of CaMKK, cancel ischemia-reperfusion stimulated D-3-HB utilization. This supports the idea that ischemia-reperfusion-stimulated D-3-HB utilization is mediated by p38 MAPK and AMPK signaling pathways. Stress that alters the AMP/ATP ratio, mitochondrial and cytosolic concentration of calcium modulates D-3-HB metabolism. Ionomycin and anisomycin modulate AMPK and p38 MAPK, respectively, without affecting the AMP/ATP ratio, and both modulators stimulate D-3-HB utilization.

Pelletier and Coderre (4) reported that prolonged pretreatment of cardiomyocytes for 16h with D-3-HB caused the partial

inhibition of DNP-stimulated AMPK and abolished stimulation by DNP of p38 MAPK. D-3-HB also partially inhibited DNP-stimulated glucose uptake in cardiomyocytes. They suggested that the inhibitory effect of D-3-HB on glucose uptake is due to the inhibitory effect of D-3-HB on AMPK / p38 MAPK activities, but they did not estimate D-3-HB utilization. It is possible that D-3-HB can limit its own utilization under certain conditions by inhibiting AMPK/p38 MAPK activities, serving as a feed-back control. However, we did not estimate AMPK/p38 MAPK activities, and the perfusion period did not exceed 2h. Therefore, we would not expect to record the effect of D-3-HB on both kinases. The citrate level is increased in hearts perfused with D-3-HB (48), and it is known that citrate inhibits AMPK phosphorylation in rat hypothalamus (49), suggesting a possible mechanism whereby D-3-HB inhibits AMPK. Moreover, acetoacetate increases the phosphorylation of extracellular signal-regulated kinase  $\frac{1}{2}$  (ERK1/2) and p38 MAPK in hepatocytes (50), and we found that DNP stimulates acetoacetate utilization in the heart (unpublished observation). It is conceivable that D-3-HB protects the cells against ATP depletion by providing NADH to the electron transport chain. D-3-HB may either limit or counteract the effect of DNP (decrease in mitochondrial membrane potential and ATP/ADP ratio) by providing a high supply of reducing equivalents to the respiratory chain, since it is oxidized directly in the mitochondrial matrix. D-3-HB further compensates for the energy deficit caused by either DNP or metabolic stress. DNP contributes to proton leakage, which keeps the cell  $\text{NAD}^+/\text{NADH}$  ratio sufficiently high and allows the required carbon metabolism to continue. It has been proposed that the high  $\text{NAD}^+/\text{NADH}$  ratio enhances AMPK activity

(51), but others findings lack any sufficient support (52).

Fasting (24 or 48h) is associated with the stimulation of cardiac D-3-HB utilization (8). AMPK is activated by fasting and is suppressed by Ara-A (53). Also, Ara-A decreased AMPK phosphorylation in the heart in response to the deprivation of glucose (54). Taken together, these findings showed that the modulation of either the AMPK or p38 MAPK signaling pathways had a role in regulating D-3-HB utilization. Our study also showed that DNP stimulated D-3-HB utilization in the isolated perfused heart is mediated by the AMPK signaling pathway, and that  $Ca^{2+}$  has a significant role in regulating D-3-HB utilization through its activation of CaMKK, which then activates AMPK. Both mechanisms, altering either the ATP/AMP or  $Ca^{2+}$  levels, could independently contribute to the enhancement of D-3-HB utilization.

We proceeded to observe that mimicking chemical hypoxia with DNP, or chemical ischemia–reperfusion with anisomycin, or activating AMPK/p38 MAPK stimulated the utilization of D-3-HB, and the inhibition of either kinases are associated with the reduction of D-3-HB utilization in the isolated perfused heart. AMPK and p38 MAPK are stimulated in response to ischemia (9, 31, 45). No-flow ischemia stimulates AMPK  $\alpha 2$  and  $\alpha 1$  activities and is most likely mediated by LKB1 (AMPKK) and CaMKK, respectively (41), and AMPK  $\alpha 2$  has a greater dependence on AMP (55). Cardiac AMPK activity is stimulated by ischemia and reperfusion (11). Since it is well known that such stressor effects are mediated by AMPK/p38 MAPK, our data supports the idea that both kinases are involved in the regulation of D-3-HB metabolism in the heart. Since PD-169316 and STO-609 abolished D-3-HB utilization

stimulated by ischemia–reperfusion, our data also support that both AMPK and p38 MAPK mediate the ischemia-reperfusion effect. We encountered a few limitations that include having not measured either the AMPK or p38 MAPK activities, and using the available selective activators and inhibitors of the both kinases.

We conclude that: DNP (an activator of both cardiac AMPK and p38 MAPK), anisomycin (a selective activator of p38 MAPK), and ionomycin (a CaMKK activator), stimulate D-3-HB utilization in heart, and this stimulation is either partially or completely abolished by selective inhibitors of the above mentioned kinases. The chemical stress may be possibly mediated by changes in  $Ca^{2+}$  concentration and /or AMP/ATP levels, through the AMPK/p38 MAPK signaling pathways. Global no-flow ischemia stimulates D-3-HB utilization possibly through the same signaling pathways. However, this needs further investigations to elucidate the involvement of the above mentioned signaling pathways.

## ACKNOWLEDGMENT

The authors would like to thank Mr. Ibn Idreas Mustafa for his technical assistance, Dr. Heba Adly for the graphics and Miss Sameerah Nazlawi for typing the manuscript. The study was supported by Umm Al-Qura University, Makkah, Saudi Arabia.

## CONFLICT OF INTEREST

Nothing to declare.

## REFERENCES

1. Stanley WC, Recchia FA, Lopaschuk GD. Myocardial substrate metabolism in the normal and failing heart. *Physiol Rev* 2005; 85: 1093-1129.
2. Sultan AMN. D-3-hydroxybutyrate metabolism in the perfused rat heart. *Mol Cell Biochem* 1988; 79: 113-118.
3. Hasselbaink DM, Glatz JFC, Luiken JJFP, Roemen THM, Van der Vusse GJ. Ketone bodies disturb fatty acid handling in isolated cardiomyocytes derived from control and diabetic rats. *Biochem* 2003; *J* 371: 753-760.
4. Pelletier A, Coderre L. Ketone bodies alter dinitrophenol-induced glucose uptake through AMPK inhibition and oxidative stress generation in adult cardiomyocytes. *Am J Physiol Endocrinol Metab* 2007; 292: E1325-E1332.
5. Stanley WC, Meadows SR, Kivilo KM, Roth BA, Lopaschuk GD.  $\beta$ -Hydroxybutyrate inhibits myocardial fatty acid oxidation in vivo independent of changes in malonyl-CoA content. *Am J Physiol Heart Circ Physiol* 2003; 285: H1626-H1631.
6. Zou Z, Sasaguri S, Rajesh KG, Suzuki R. dl-3-Hydroxybutyrate administration prevents myocardial damage after coronary occlusion in rat hearts. *Am J Physiol Heart Circ Physiol* 2002; 283: H1968-H1974.
7. Sultan AMN. The effects of chronic diabetes and physiological insulin concentration on ketone bodies metabolism in the heart. *Diabetes Res* 1994; 27: 47-60.
8. Sultan AMN. The effect of fasting on D-3-hydroxybutyrate metabolism in the perfused rat heart. *Mol Cell Biochem* 1990; 93: 107-118.
9. Russell RR 3rd, Li J, Coven DL, Pypaert M, Zechner C, Palmeri M, Giordano FJ, Mu J, Birnbaum MJ, Young LH. AMP-activated protein kinase mediates ischemic glucose uptake and prevents postischemic cardiac dysfunction, apoptosis, and injury. *J Clin Invest* 2004; 114: 495-503.
10. Young LH, Li J, Baron SJ, Russell RR. AMP-activated protein kinase: A key stress signaling pathway in the heart. *Trends Cardiovasc Med* 2005; 15: 110-8.
11. Kudo N, Barr AJ, Barr RL, Desai S, Lopaschuk GD. High rates of fatty acid oxidation during reperfusion of ischemic hearts are associated with a decrease in malonyl-CoA levels due to an increase in 5'-AMP-activated protein kinase inhibition of acetyl-CoA carboxylase. *J Biol Chem* 1995; 270: 17513-17520.
12. Pelletier A, Joly E, Prentki M, Coderre L. Adenosine 5'-monophosphate-activated protein kinase and p38 mitogen-activated protein kinase participate in the stimulation of glucose uptake by dinitrophenol in adult cardiomyocytes. *Endocrinology* 2005; 146: 2285-2294.
13. Russell RR 3rd, Bergeron R, Shulman GI, Young LH. Translocation of myocardial GLUT-4 and increased glucose uptake through activation of AMPK by AICAR. *Am J Physiol Heart Circ Physiol* 1999; 277: H643-H649.

14. Sambandam N, Lopaschuk GD. AMP-activated protein kinase (AMPK) control of fatty acid and glucose metabolism in the ischemic heart. *Prog Lipid Res* 2003; 42: 238-256.
15. Fisher RB, O'Brien JA. The effects of endogenous and added insulin on the time-course of glucose uptake by the isolated perfused rat heart. *Q J Exp Physiol Cogn Med Sci* 1972; 57:176-191.
16. Williamson DH, Mellanby J. D-(-)-3-hydroxybutyrate. In: Hans Ulrich Bergmeyer (ed). *Methods of Enzymatic Analysis*. 1974; Vol 4. pp (1836-1839) Academic Press.
17. Mellanby J, Williamson DH. Acetoacetate. In: Hans Ulrich Bergmeyer (ed). *Methods of Enzymatic Analysis*. 1974; Vol 4, pp (1841-1843) Academic Press.
18. Newby AC, Holmquist CA, Illingworth J, Pearson JD. The control of adenosine concentration in polymorph nuclear leucocytes, cultured heart cells and isolated perfused heart from the rat. *Biochem J* 1983; 214: 317-323.
19. Musi N, Hayashi T, Fujii N, Hirshman MF, Witters LA, Goodyear LJ. AMP-activated protein kinase activity and glucose uptake in rat skeletal muscle. *Am J PhysiolEndocrinolMetab*2001; 280: E677-E684.
20. Morgan AJ, Jacob R. Ionomycin enhances Ca<sup>2+</sup> influx by stimulating store-regulated cation entry and not by a direct action at the plasma membrane. *Biochem J* 1994; 300: 665-672.
21. Hawley SA, Pan DA, Mustard KJ, Ross L, Bain J, Edelman AM, Frenguelli BG, Hardie DG. Calmodulin-dependent protein kinase kinase-β is an alternative upstream kinase for AMP-activated protein kinase. *Cell Metab*2005; 2: 9-19.
22. Hurley RL, Anderson KA, Franzone JM, Kemp BE, Means AR, Witters LA. The Ca<sup>2+</sup>/Calmodulin-dependent protein kinase kinases are AMP-activated protein kinase kinases. *J BiolChem* 2005; 280(32): 29060-29066.
23. Tokumitsu H, Inuzuka H, Ishikawa Y, Ikeda M, Saji I, Kobayashi R. STO-609, a specific inhibitor of the Ca<sup>2+</sup>/Calmodulin-dependent protein kinase kinase. *J BiolChem* 2002; 277: 15813-15818.
24. Hudman D, Rainbow RD, Lawrence CL, Standen NB. The origin of calcium overload in rat cardiac myocytes following metabolic inhibition with 2,4-dinitrophenol. *J Mol Cell Cardiol* 2002; 34: 859-871.
25. Kang S, Kim N, Joo H, Youm JB, Park WS, Warda M, Kim H, Cuong DV, Kim T, Kim E, Han J. Changes of cytosolic Ca<sup>2+</sup> under metabolic inhibition in isolated rat ventricular myocytes. *Korean J PhysiolPharmacol* 2005; 9: 291-298.
26. Rodrigo GC, Lawrence CL, Standen NB. Dinitrophenol pretreatment of rat ventricular myocytes protects against damage by metabolic inhibition and reperfusion. *J Mol Cell Cardiol* 2002; 34: 555-569, 2002.
27. Alekseev AE, Gomez LA, Aleksandrova LA, Brady PA, Terzic A. Opening of cardiac sarcolemmal KATP channels by dinitrophenol separate from metabolic inhibition. *J*

- MembrBiol* 1997; 157: 203-214.
28. Jilkina O, Kuzio B, Grover GJ, Kupriyanov VV. Effects of K(ATP) channel openers, P-1075, pinacidil, and diazoxide, on energetics and contractile function in isolated rat hearts. *J Mol Cell Cardiol* 2002; 34: 427-440.
  29. Sasaki N, Sato T, Marbán E, O'Rourke B. ATP consumption by uncoupled mitochondria activates sarcolemmal K(ATP) channels in cardiac myocytes. *Am J Physiol Heart CircPhysiol* 2001; 280: H1882-H1888.
  30. Sukhodub A, Jovanović S, Du Q, Budas G, Clelland AK, Shen M, Sakamoto K, Tian R, Jovanović A. AMP-activated protein kinase mediates preconditioning in cardiomyocytes by regulating activity and trafficking of sarcolemmal ATP-sensitive K<sup>+</sup> channels. *J Cell Physiol* 2007; 210: 224-236.
  31. Li J, Miller EJ, Ninomiya-Tsuji J, Russell RR 3rd, Young LH. AMP-activated protein kinase activates p38 mitogen-activated protein kinase by increasing recruitment of p38 MAPK to TAB1 in the ischemic heart. *Circ Res* 2005; 97: 872-879.
  32. KummerJL, RaoPK,HeidenreichKA. Apoptosis induced by withdrawal of trophic factors is mediated by p38 mitogen-activated protein kinase. *J BiolChem* 1997; 272: 20490-20494.
  33. Konrad D, Rudich A, Bilan PJ, Patel N, Richardson C, Witters LA, Klip A. Troglitazone causes acute mitochondrial membrane depolarisation and an AMPK-mediated increase in glucose phosphorylation in muscle cells. *Diabetologia* 2005; 48: 954-966.
  34. Ray J, Noll F, Daut J, Hanley PJ. Long-chain fatty acids increase basal metabolism and depolarize mitochondria in cardiac muscle cells. *Am J Physiol Heart CircPhysiol* 2002; 282: H1495-H1501.
  35. Dyck JR, Kudo N, Barr AJ, Davies SP, Hardie DG, Lopaschuk GD. Phosphorylation control of cardiac acetyl-CoA carboxylase by cAMP-dependent protein kinase and 5'-AMP activated protein kinase. *Eur J Biochem* 1999; 262: 184-190.
  36. Stapleton D, Mitchelhill K I, Gao G, Widmer J, Michell B J, Teh T, House C M, Fernandez C S, Cox T, Witters L A, Kemp BE. Mammalian AMP-activated protein kinase subfamily. *J BiolChem* 1996; 271: 611-614.
  37. Hayashi T, Hirshman MF, Fujii N, Habinowski SA, Witters LA, Goodyear LJ. Metabolic Stress and Altered Glucose Transport activation of AMP-activated protein kinase as a unifying coupling mechanism. *Diabetes* 2000; 49: 527-531.
  38. Parkinson FE, Geiger JD. Effects of iodotubercidin on adenosine kinase activity and nucleoside transport in DDT1 MF-2 smooth muscle cells. *J PharmacolExpTher* 1996; 277: 1397-1401.
  39. Aymerich I, Foufelle F, Ferré P, Casado FJ, Pastor-Anglada M. Extracellular adenosine activates AMP-dependent protein kinase (AMPK). *J Cell Sci* 2006; 119: 1612-1621.
  40. Woods A, Dickerson K, Heath R, Hong SP, Momcilovic M, Johnstone SR, Carlson M, Carling D. Ca<sup>2+</sup>/Calmodulin-dependent protein

- kinase kinase- $\beta$  acts upstream of AMP-activated protein kinase in mammalian cells. *Cell Metab* 2005; 2: 21-33.
41. Sakamoto K, Zarrinpashneh E, Budas GR, Pouleur AC, Dutta A, Prescott AR, Vanoverschelde JL, Ashworth A, Jovanović A, Alessi DR, Bertrand L. Deficiency of LKB1 in heart prevents ischemia-mediated activation of AMPK $\alpha_2$  but not AMPK $\alpha_1$ . *Am J PhysiolEndocrinolMetab* 2006; 290: E780-E788.
  42. Da Silva CG, Jarzyna R, Specht A, Kaczmarek E. Extracellular nucleotides and adenosine independently activate AMP-activated protein kinase in endothelial cells: involvement of P2 receptors and adenosine transporters. *Circ Res* 98: e39-e47, 2006.
  43. Chai W, Wu Y, Li G, Cao W, Yang Z, Liu Z. Activation of p38 mitogen-activated protein kinase abolishes insulin-mediated myocardial protection against ischemia-reperfusion injury. *Am J PhysiolEndocrinolMetab* 2008; 294: E183-E189.
  44. Armstrong SC. Protein kinase activation and myocardial ischemia/reperfusion injury. *Cardiovas Res* 2004; 61: 427-436.
  45. Bogoyevitch MA, Gillespie-Brown J, Ketterman AJ, Fuller SJ, Ben-Levy R, Ashworth A, Marshall CJ, Sugden PH. Stimulation of the stress-activated mitogen-activated protein kinase subfamilies in perfused heart. p38/RK mitogen-activated protein kinases and c-Jun N-terminal kinases are activated by ischemia/reperfusion. *Circ Res* 1996; 79: 162-173.
  46. Bogoyevitch MA, Ketterman AJ, Sugden PH. Cellular stresses differentially activate c-Jun N-terminal protein kinases and extracellular signal-regulated protein kinases in cultured ventricular myocytes. *J BiolChem* 1995; 270: 29710-29717.
  47. Jacquet S, Zarrinpashneh E, Chavey A, Ginion A, Leclerc I, Viollet B, Rutter GA, Bertrand L, Marber MS. The relationship between p38 mitogen-activated protein kinase and AMP-activated protein kinase during myocardial ischemia. *Cardiovascular Research* 2007; 76 : 465-472.
  48. Sato K, Kashiwaya Y, Keon CA, Tsuchiya N, King MT, Radda GK, Chance B, Clarke K, Veech RL. Insulin, ketone bodies, and mitochondrial energy transduction. *FASEB J* 1995; 9: 651-658.
  49. Stoppa GR, Cesquini M, Roman EA, Prada PO, Torsoni AS, Romanatto T, Saad MJ, Velloso LA, Torsoni MA. Intracerebroventricular injection of citrate inhibits hypothalamic AMPK and modulates feeding behavior and peripheral insulin signaling. *J Endocrinol* 2008; 198: 157-168.
  50. Abdelmegeed MA, Kim SK, Woodcroft KJ, Novak RF. Acetoacetate activation of extracellular signal-regulated kinase 1/2 and p38 mitogen-activated protein kinase in primary cultured rat hepatocytes: role of oxidative stress. *J PharmacolExTher* 2004; 310: 728-736.
  51. Rafaeloff-Phail R, Ding L, Conner L, Yeh WK, McClure D, Guo H, Emerson K, Brooks H. Biochemical regulation of mammalian AMP-

- activated protein kinase activity by NAD and NADH. *J BiolChem* 2004; 279: 52934-52939.
52. Suter M, Riek U, Tuerk R, Schlattner U, Wallimann T, Neumann D. Dissecting the role of 5'-AMP for allosteric stimulation, activation, and deactivation of AMP-activated protein kinase. *J BiolChem* 2006; 281: 32207-32216.
53. An D, Pulinilkunnil T, Qi D, Ghosh S, Abrahani A, Rodrigues B. The metabolic "switch" AMPK regulates cardiac heparin-releasable lipoprotein lipase. *Am J PhysiolEndocrinolMetab* 2005; 288: E246-E253.
54. Matsui Y, Takagi H, Qu X, Abdellatif M, Sakoda H, Asano T, Levine B, Sadoshima J. Distinct roles of autophagy in the heart during ischemia and reperfusion: Roles of AMP-activated protein kinase and Beclin 1 in mediating autophagy. *Circ Res* 2007; 100: 914-922.
55. Salt I, Celler JW, Hawley SA, Prescott A, Woods A, Carling D, Hardie DG. AMP-activated protein kinase: greater AMP dependence and preferential nuclear localization, of complexes containing the  $\alpha_2$  isoform. *BiolChem J* 1998; 334: 177-187.

## Case report

# A case of Kikuchi-Fujimoto's disease in a 31 year old Saudi female patient with lupus nephritis

Ekhlas Bardisi 1, Hani Almoallim 1, Hassan Sayadi 3

1 Medical Intern, Department of Medicine, King Faisal Specialist Hospital & Research center (KFSH&RC), Jeddah,

1 Medical College, Umm Al-Qura University, Makkah, Saudi Arabia, Consultant Rheumatologist, KFSH&RC, Jeddah

3 Consultant Pathologist, KFSH&RC, Jeddah

### Correspondence :

**Dr. Hani Almoallim**

Associate Professor, Medical College, Umm Alqura University

P.O. Box 1821, Jeddah 21441, Saudi Arabia

hanialmoallim@hotmail.com

## الاشكال المتعددة لجين الجلوتاثيون س – ترانسفيريز ومخاطر الإصابة بسرطان قولون المستقيم في السعوديين

د. الاخلاص البرديسي 1، د. هاني معلم 2، د. حسن الصيادي 3  
متدرب الطبية، قسم الطب ومستشفى الملك فيصل التخصصي ومركز الأبحاث (مستشفى الملك فيصل التخصصي)، جدة  
1، كلية الطب، جامعة أم القرى، مكة المكرمة، المملكة العربية السعودية، أمراض الروماتيزم استشاري، مستشفى الملك فيصل التخصصي بجدة<sup>2</sup>، علم الأمراض استشاري، مستشفى الملك فيصل التخصصي بجدة<sup>3</sup>.

### الملخص

يعتبر مرض كاكوشي فيوجيموتو مرضاً نادراً ينتهي تلقائياً مع علاقة موثقة بمرض الذئبة الحمراء الحمامي الجهازية. نحن نوثق هنا في هذا التقرير حالة من هذا المرض بناء على خزعة أخذت من غدة لمفاوية من امرأة سعودية عمرها 31 عاماً مع تشخيص سابق بالتهاب الذئبة الحمامية الكلوي من الدرجة الرابعة. لقد ظهر المرض لديها بحرارة وإنتفاخ في الغدد اللمفاوية الباطية مع قلة كريات الدم البيضاء. لقد أخذت المريضة مضادات حيوية وريدية ولكن المريضة تحسنت بصورة تلقائية

### ABSTRACT

#### Background:

Kikuchi-Fujimoto's disease (KFD) is a rare benign self-limited disease with reported relation to systemic lupus erythematosus (SLE). We report a case of KFD based on a lymph node biopsy in a 31 year old Saudi female patient with an established diagnosis of stage IV lupus nephritis. She presented with fever, axillary lymphadenopathy, and neutropenia. Intravenous antibiotic was considered as a case of febrile neutropenia. The patient recovered spontaneously.

#### Keywords:

**K**ikuchi-Fujimoto's disease (KFD) or histiocytic necrotizing lymphadenitis is a benign, self-limited disease of unknown etiology that affects mainly young women. It presents with localized lymphadenopathy, predominantly in the cervical region, less commonly axillary and mesenteric lymphadenopathy accompanied by fever and leukopenia in up to 50% of the cases [1, 2]. KFD has been reported in association with systemic lupus erythematosus (SLE) [1-4]; the relation between KFD and SLE is not yet completely understood and remains complex. SLE may be present before, at the same time, or after the clinical appearance of KFD [1, 2, 5]. We described a case of KFD in a 31 year old Saudi female patient with an established diagnosis of stage IV lupus nephritis.

## CASE REPORT

We reported a 31 year old Saudi female patient who is a known case of SLE diagnosed 16 years ago (1994). She presented at that time with fever, easy fatigability, arthralgia and generalized bodyache. Investigations revealed 2+ proteins in the urine; speckled ANA (titer 1:1160), positive anti-ds-DNA antibodies at 347 IU/ml (normal range 0 – 18 IU/mL), positive anti-Sm/RNP, anti-SSA/Ro antibodies as well as low complement levels (C3, C4). She was started on prednisolone, hydroxychloroquine, azothioprine and calcium and vitamin D. She was regularly followed in our center since 2001. The patient was evaluated in 2007 due to nephrotic range proteinuria of more than 6g/24 hour. Laboratory investigations revealed speckled ANA pattern (titer 1:2640), positive anti-DNA at 813 IU/ml and

## INTRODUCTION

hypocomplementemia with negative anti-phospholipids antibodies titer. Renal biopsy in February 2007 was characterized by stage IV lupus nephritis. The condition was treated with mycophenolate mofetil (1 gram orally twice a day), tapering dose of prednisolone, hydroxychloroquine and calcium and vitamin D supplements. Proteinuria initially regressed to 1.65 g/day but with poor medical compliance, this, unfortunately, resulted in flare up of her disease.

In August 2008, repeated renal biopsy again showed class IV lupus nephritis with membranous component. She was treated with six doses of cyclophosphamide from September 2008 to February 2009. She was maintained afterwards on azothioprine and hydroxychloroquine.

Due to persistent leukopenia (WBC 1.5 x 10<sup>9</sup>/L) azothioprine was discontinued in outpatient rheumatology clinic in her follow up visit in April 2010. She was admitted to the hospital in May 2010 with 1-week history of high grade fever (39-40°C) and persistent leukopenia despite stopping azothioprine. Her fever was continuous with minimal response to antipyretics. It was associated with sweats, chills, and rigors. There was no history suggestive of any source of infection. She denied history of joint pains and swellings. There was no history of alopecia, mouth or genital ulcers, malar rash or skin rash and no history of weight loss or loss of appetite.

On physical examination, she was in general good condition but with temperature of 39.1°C, blood pressure of 121/63 mmHg, heart rate of 88 beat/min and respiratory rate of 20 breath/min, O<sub>2</sub> saturation 98% on room air. She had tender, right axillary lymphadenopathy. Cardiovascular, respiratory and abdominal examinations

were unremarkable. There were no signs of arthritis.

The laboratory investigations showed WBC of  $1.52 \times 10^9/L$ , hemoglobin of 100 g/l, platelets of 161,000 /mm<sup>3</sup>, absolute neutrophilic count (ANC) of  $0.69 \times 10^3/\mu L$ , dropped to below  $0.50 \times 10^3/\mu L$  and lymphocytes of 44.4%, erythrocyte sedimentation rate (ESR) of 47 mm/h, C-reactive protein (CRP) of 36.1 mg/l. Renal and hepatic profiles were normal. Urinalysis was normal except of 2+ protein that was similar to previous findings. All cultures including blood and urine were all negative. Serological tests for Brucella, cytomegalovirus (CMV), Epstein - Barr virus (EBV), malaria, hepatitis A, B, C, were all negative. ANA was positive and also Anti-ds-DNA was 39.3 IU/ml with normal complement level C3 of 1.2 g/l and C4 of 0.16 g/l. CT of chest, abdomen and pelvis showed no evidence of fluid collection with hepatosplenomegaly and significant bilateral axillary lymphadenopathy more on the right. Right axillary lymph node excisional biopsy was done and showed histiocytic necrotizing lymphadenitis consistent with KFD {figure 1, 2, 3}.

The patient was treated as a case of febrile neutropenia with intravenous antibiotics for 7 days. Her symptoms, signs including WBC count improved spontaneously. She was discharged in good condition on plaquenil, calcium, and vitamin D. She developed post operative wound infection; abscess was drained at site of axillary lymph node biopsy with daily dressing. Her WBC count reached  $2.38 \times 10^9/L$  two weeks after discharge at time of outpatient follow up visit. This count continued to improve and reached  $4.0 \times 10^9/L$  a month later. She was put back on

azathioprine with normal WBC count for 9 months after initial presentation.

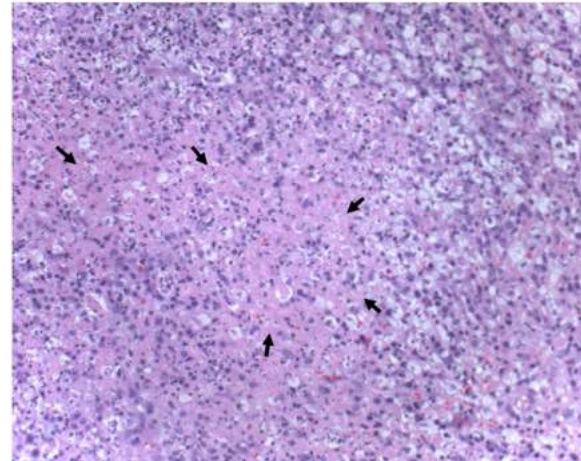


Figure 1: It shows an area of patchy necrosis (arrows) with increased number of histiocytes in the paracortical regions (hematoxylin-eosin, original magnification x 200).

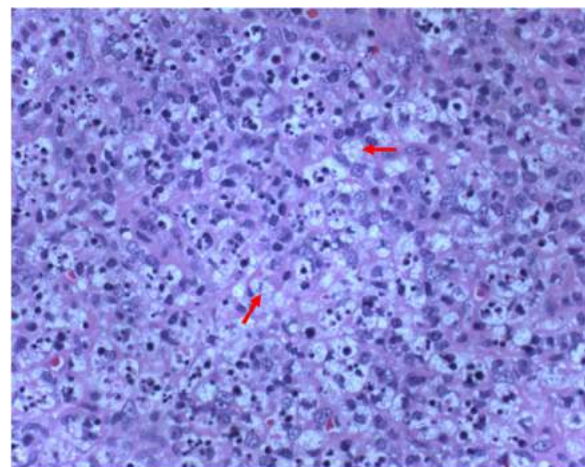


Figure 2: high power view of an expanded paracortical area showing numerous histiocytes (arrows), many of which are necrotic (hematoxylin-eosin, original magnification x 400).

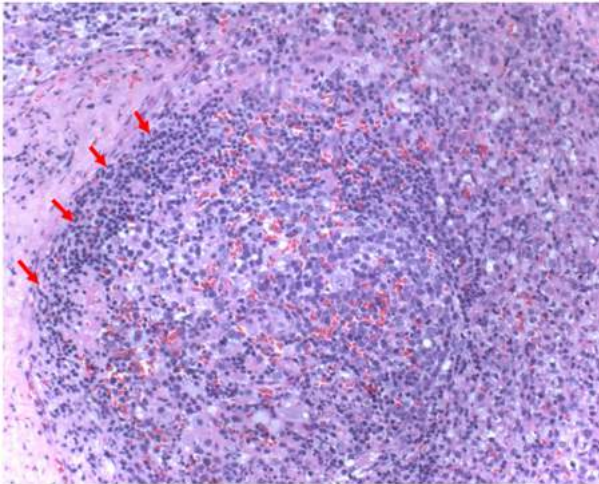


Figure 3: this slide shows only rare residual lymphoid follicles (arrows) with reactive germinal center are seen (hematoxylin-eosin, original magnification x 200).

## DISCUSSION

KFD or histiocytic necrotizing lymphadenitis, was originally described in Japan in 1972 by Kikuchi [6] and Fujimoto et al. [7]. It has been reported in several countries since then [8] including Saudi Arabia [9] but predominantly in Asia.

It often affects young adult women [9, 13-15]. Pathogenesis of this disease is still not fully understood. It is proposed that the primary event may be the activation of T lymphocytes and histiocytes. Proliferating T cells enter the cycle of apoptosis, which may form the areas of necrosis in lymph nodes and then the cellular debris is removed by histiocytes [5, 16, 17]. Certain microorganisms (EBV, herpes human 6 virus, Toxoplasma, parvovirus B19, CMV, Brucella, Yersinia enterocolitica and parainfluenza virus) have been suggested as the causative agents of the disease, initiating a hyper-immune response of the T cells and histiocytes to the infectious agents. However, none of these possibilities have been

definitively proven [5, 12, 17]. An autoimmune origin has also been suggested due to a number of cases in which SLE was diagnosed previously, simultaneously or after KFD, demonstrating a strong association [1, 2]. In most of the cases the diagnosis of KFD was made before or at the same time of the diagnosis of SLE, However, In our case the diagnosis of KFD was made years after the diagnosis of SLE. It is also noted that our patient received prolonged courses of immunosuppressant medications including mycophenolate mofetil, and later 6 cycles of cyclophosphamide, she was then placed on azathioprine and hydroxychloroquine. Can we consider the prolonged use of immunosuppressant medications a risk factor for KFD in a well established SLE with lupus nephritis? This is a concern that might be raised; however, there is no literature suggestive of this observation. It clearly warrants further evaluation.

Clinically, a unilateral cervical lymphadenopathy in KFD is observed [10, 13, 15, 16], but enlargement of lymph nodes in other regions may also be seen, sometimes in the form of generalized lymphadenopathy [10, 11, 14]. The affected lymph nodes vary in size from 0.5 to 7 cm of diameter [14] and may be tender or painful [13, 14, 16, 17]. The other, most common clinical symptoms of this disease are low-grade fever [10, 14-17], arthralgia and variety of skin rashes that usually precede lymphadenopathy [10, 13]. However, non-specific symptoms, e.g. weakness, night sweats, weight loss, diarrhea, anorexia, chills, nausea, vomiting, chest and abdominal pain have also been reported [10, 13, 16]. Sometimes splenomegaly and hepatomegaly are encountered [10, 13] like what we encountered in the case presented here.

Laboratory findings are not specific including elevated ESR, leukopenia with mild lymphocytosis and atypical lymphocytes [10, 13-17]. Moreover, in less than 5% of cases leukocytosis is found [11, 14].

The disease is generally diagnosed on the basis of an excisional biopsy of affected lymph nodes. Characteristic histopathological findings of KFD include irregular paracortical areas of coagulative necrosis with abundant karyorrhectic debris, which can distort the nodal architecture, and large number of different types of histiocytes at the margin of the necrotic areas [2]. The karyorrhectic foci are formed by various cellular types, predominantly histiocytes and plasmacytoid monocytes but also immunoblasts and small and large lymphocytes. Neutrophils are characteristically absent, and plasma cells are either absent or scarce. The pathological findings in our case include abnormal nodal architecture; there is extensive expansion of the paracortical regions with numerous histiocytes, many of which are necrotic and contain nuclear debris. In addition, there are patchy areas of necrosis; also there are several reactive lymphocytes and immunoblasts with occasional plasma cells in the paracortical regions.

KFD tends to resolve spontaneously within 1 week to 3 years [15, 16] but it may also recur in about 3% of cases [11, 13, 14]. In the cases in which KFD was diagnosed after or concomitantly with SLE, an obvious tendency was observed to adopt the use of corticosteroids, associated or not with hydroxychloroquine, as a standard treatment [5, 12]. On the other hand, when KFD is diagnosed before SLE, it is considered a clinically isolated entity and generally there

is no need for treatment due to its benign and self-limited nature, with spontaneous resolution in weeks or months [3, 4, 18], our patient was treated as a case of febrile neutropenia with intravenous antibiotics for 7 days. Her symptoms, signs, and WBC count improved spontaneously.

In conclusion, although KFD is a self-limited condition, it can rarely be associated with SLE. We described a case of SLE with stage IV lupus nephritis that developed clinically and pathologically new clinical and pathological findings that was explained by KFD. Supportive measures were considered, and the disease resolved spontaneously. Is the prolonged use of immunosuppressant medications a risk factor for KFD in SLE patients?

## REFERENCES

1. Kucukardali Y, Solmazgul E, Kunter E, Oncul O, Yildirim S, Kaplan M. Kikuchi-Fujimoto Disease: analysis of 244 cases. *Clin Rheumatol.* 2007 Jan;26(1):50-4.
2. Santana A, Lessa B, Galvão L, Lima I, Santiago M. Kikuchi-Fujimoto's disease associated with systemic lupus erythematosus: case report and review of the literature. *Clin Rheumatol.* 2005 Feb;24(1):60-3.
3. Litwin MD, Kirkham B, Henderson DR, Milazzo SC. Histiocytic necrotising lymphadenitis in systemic lupus erythematosus. *Ann Rheum Dis.* 1992 Jun;51(6):805-7.
4. El-Ramahi KM, Karrar A, Ali MA. Kikuchi disease and its association with systemic lupus erythematosus. *Lupus.* 1994 Oct;3(5):409-11.

5. Martínez-Vázquez C, Hughes G, Bordon J, Alonso-Alonso J, Anibarro-Garcia A, Redondo-Martínez E, Touza-Rey F. Histiocytic necrotizing lymphadenitis, Kikuchi-Fujimoto's disease, associated with systemic lupus erythematosus. *QJM*. 1997 Aug;90(8): 531-3.
6. Kikuchi M. Lymphadenitis showing focal reticulum cell hyperplasia with nuclear debris and phagocytes: a clinicopathological study. *Acta Hematol Jpn* 1972; 35: 379-80 .
7. Fujimoto Y, Kojima Y, Yamaguchi K. cervical sub acute necrotizing lymphadenitis. *Naika* 1972. 20:920-7
8. Dorfman RF, Berry GJ. Kikuchi's histiocytic necrotizing lymphadenitis: an analysis of 108 cases with emphasis on differential diagnosis. *Semin Diagn Pathol*. 1988 Nov;5(4):329-45.
9. Kucukardali Y, Solmazgul E, Kunter E, Oncul O, Yildirim S, Kaplan M. Kikuchi-Fujimoto Disease: analysis of 244 cases. *Clin Rheumatol*. 2007 Jan;26(1):50-4.
10. Adhikari RC, Sayami G, Lee MC, Basnet RB, Shrestha PK, Shrestha HG. Kikuchi-Fujimoto disease in Nepal: a study of 6 cases. *Arch Pathol Lab Med*. 2003 Oct;127(10):1345-8.
11. Snow RL, Ferry JA. Case 5-1997—a 24-year-old woman with cervical lymphadenopathy, fever, and leukopenia. *N Engl J Med*. 1997 Feb 13;336(7):492-9.
12. Danowski A, Bica B, Baptista R, Nentzinsky W, Azavedo MN. Linfadenite de Kikuchi associada ao lupus eritematosos sistêmico. *Rev Bras Reumatol* 2003 43:58-61
13. Charalabopoulos K, Papatimneou V, Charalabopoulos A, Chaidos A, Bai M, Bourantas K, Agnantis N. Kikuchi-Fujimoto disease in Greece. A study of four cases and review of the literature. *In Vivo*. 2002 Sep-Oct;16(5):311-6.
14. Kuo TT. Kikuchi's disease (histiocytic necrotizing lymphadenitis). A clinicopathologic study of 79 cases with an analysis of histologic subtypes, immunohistology, and DNA ploidy. *Am J Surg Pathol*. 1995 Jul;19(7):798-809
15. Tumiati B, Bellelli A, Portioli I, Prandi S. Kikuchi's disease in systemic lupus erythematosus: an independent or dependent event? *Clin Rheumatol*. 1991 Mar;10(1):90-3.
16. Papaioannou G, Speletas M, Kaloutsi V, Pavlitou-Tsiontsi A. Histiocytic necrotizing lymphadenitis (Kikuchi-Fujimoto disease) associated with antiphospholipid syndrome: case report and literature review. *Ann Hematol*. 2002 Dec;81(12):732-5 .
17. Menasce LP, Banerjee SS, Edmondson D, Harris M. Histiocytic necrotizing lymphadenitis (Kikuchi-Fujimoto disease): continuing diagnostic difficulties. *Histopathology*. 1998 Sep;33(3):248-54.
18. Vilá LM, Mayor AM, Silvestrini IE. Therapeutic response and long-term follow-up in a systemic lupus erythematosus patient presenting with Kikuchi's disease. *Lupus*. 2001;10(2):126-8.

## Case report

# Oropharyngeal choristoma in association with congenital hypoplasia of depressor angularis oris muscle in a neonate

Helal Almalki 1, Najia Al-Hojaili 1, Mohammad Nasim Khan 2\*, Khalid Bader 3, Ibrahim Kotobi 1, Habeeb Ibrahim 4

Department of Pediatrics1, Department of ENT3, Department of Histopathology4 Maternity and Children Hospital, Makkah. Department of Pediatrics2, Umm-Al-Qura University, Makkah, Kingdom of Saudi Arabia

### Correspondence :

**Dr. Mohammad Nasim Khan**

Assistant Professor

Department of Pediatrics,

Um-Alqura University, Makkah

Kingdom of Saudi Arabia

Email: nasimkhan00@hotmail.com

## كورستوما هو عبارة عن تجمع لأنسجة طبيعية في أماكن شاذة بما يشبه الأورام الحميدة.

د. هلال المالكي1، ناجية ألهجاني1، محمد نسيم خان2، خالد بدر3، إبراهيم كتيبي1، حبيب إبراهيم4  
قسم طب الأطفال1، قسم الأنف والحنجرة2، قسم التشريح4 المرضي مستشفى الولادة والأطفال بمكة المكرمة. قسم طب  
الأطفال2، جامعة أم القرى، مكة المكرمة، المملكة العربية السعودية

### المخلص

وتعتبر الكورستوما المختلط في الفم والبلعوم عند حديثي الولادة نادر الحدوث. وقد تم ذكر بعض حالات التشوهات الولادية مثل شراع الحنك والشندق مترافقة مع الكورستوما في الأدب الطبي. نقدم هنا، حسب علمنا، أول حالة كورستوما مختلطه عند حديث ولاده مترافقه مع نقص تصنع خلقي في العضلة الخافضة لزاوية الفم.

## ABSTRACT

### Background:

Choristoma is a benign tumor- like growth consisting of an aggregate of histologically normal tissue, which occurs in an aberrant location. Mixed choristomas of oropharynx in a neonate are rare lesions. Many congenital anomalies like cleft palate, macrostomia has been reported in literature with choristoma. To the best of our knowledge, we present here the first reported case of mixed oropharyngeal choristoma in a neonate associated with congenital hypoplasia of depressor angularis oris muscle.

**Keywords:** Choristoma, depressor angularis oris muscle, mixed, oropharyngeal

## INTRODUCTION

**C**horistoma is a benign tumor-like growth consisting of an aggregate of microscopically normal cells or tissues which occurs in aberrant locations (1). It should be differentiated from hamartoma, which are tumor-like malformations composed of focal overgrowth of mature normal cells found at their normal location. Choristoma of head and neck region is being reported at various locations like nasopharynx, oropharynx, hypopharynx, and middle ear (2, 3). It is composed of following tissue types: glial, cartilage, osseous, salivary gland, thyroid, respiratory mucosa and gastrointestinal mucosa (4).

Most cases of choristoma are reported in infants and children by 2 years of age, with an age range of newborn to 28 years with male to female ratio off 3:2 (5, 6). However mixed choristomas of oropharynx in a neonate are rare occurrence. Their clinical presentation depends on their locations. Most cases of choristoma are asymptomatic but at times it can present with distressing clinical symptoms or may start growing rapidly, mimicking malignancy. As the lesion is completely curable, the importance of early diagnosis and appropriate management in such cases is emphasized.

Many congenital anomalies like cleft palate, ectopic pancreas in palate, macrostomia, prognathic mandible has been reported in literature with oropharyngeal choristoma (7, 8).

Congenital hypoplasia of depressor angularis oris muscle (CHDAOM) is one of the rare causes of asymmetric crying facies in newborn. It is usually associated with cardiac, gastro-intestinal, genito-urinary anomalies and other malformations (9).

To the best of our knowledge, we are reporting here the first case of mixed

oropharyngeal choristoma in a neonate in association with CHDAOM.

## CASE REPORT

Five days old baby girl was transferred to the Maternity and Children Hospital in Makkah Kingdom of Saudi Arabia in November 2014 for evaluation of respiratory distress, inability to swallow and cyanosis during feeding. She was the product of full term normal vaginal delivery with no perinatal complications. The mother was gestational diabetic and received Insulin during pregnancy. There was no consanguinity between parents and no family h/o any congenital anomaly or exposures to any radiation during pregnancy. Apgar scores were 6 at 1 minute and 8 at 5 minutes.

Physical examination revealed an alert and active baby. She had vigorous cry and was able to close her eyes satisfactorily. The face was symmetrical while the neonate was quiet or sleeping. However there was obvious deviation of angle of the mouth to the right side during crying (due to CHDAOM). Baby weighed 2.3 kg, had head circumference of 33 cm and length of 47 cm. Intra oral examination was unremarkable.

Brain CT showed mild hypodensity of periventricular area, cortical sulci with normal limits. No dilated ventricles. Neck CT with contrast revealed normal appearance of the supra, infra and glottis regions, no focal thickening or masses, normal appearance of the cartilaginous frame work of the larynx, normal appearance of airway. MRI neck without contrast exhibited well defined lobulated mass lesion within the oropharynx encroaching on the lumen. It measured about 0.6X0.8X 2 cm. The lesion displayed

intermediate T<sub>1</sub>, LowT<sub>2</sub> and low STIR signals. (5)

Video fluoroscopy for swallowing study was performed and baby was found to have oropharyngeal dysphagia according to the following observations:

- inadequate oral propulsion due to reduced labial tension, reduced buccal tension, reduced tongue control ( coordination)
- weak or ineffective pharyngeal swallow with incomplete bolus clearance due to alteration of hypopharynx structures by the posterior pharyngeal wall mass and
- contrast esophagus: No evidence of fistula

Echocardiograph revealed mild coarctation of aorta

Endoscopic examination revealed lobulated, pedunculated mass extending from uvula involving the oropharynx (**Figure 1**).



**Figure (1):** Mass measured 1.5x1cm protruding from uvula and filling the oral cavity

Trans-oral complete excision of the mass was performed using bipolar electrocautery. Gross examination of specimen showed single polypoid grey tanned mucosa covered mass, firm in consistency measuring 1.5X1 cm.

Microscopic examination revealed a well – defined growth lined by simple columnar epithelium, and surrounded by stratified and

pseudostratified squamous epithelium. The subepithelial tissue shows mixture of haphazardly arranged gastric, intestinal, hepatic, and neuronal tissues, (**Figure 2**).

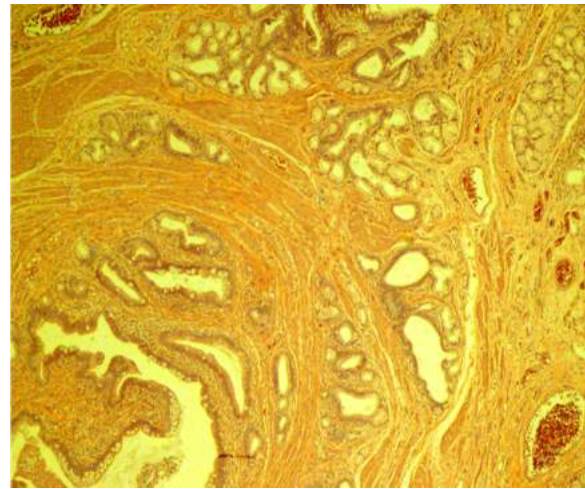


**Figure (2):** Lower power view of the choristoma showing mixture of gastric and intestinal tissues embedded between smooth muscle fibers

Immunohistochemical staining showed Hepatocytes specific antigen (HAS) positive in hepatic tissue (**Figure 4**), S-100 protein shows positive neuronal tissue (**Figure 3**), Smooth Muscle Actin (SMA) positive for smooth muscle fibers. Based on the findings of histopathology and Immunohistochemical staining, diagnosis of mixed choristoma was confirmed. Baby showed marked clinical improvement after complete excision of the mass. Her respiratory distress subsided; the attack of cyanosis disappeared and started sucking oral feeds well.

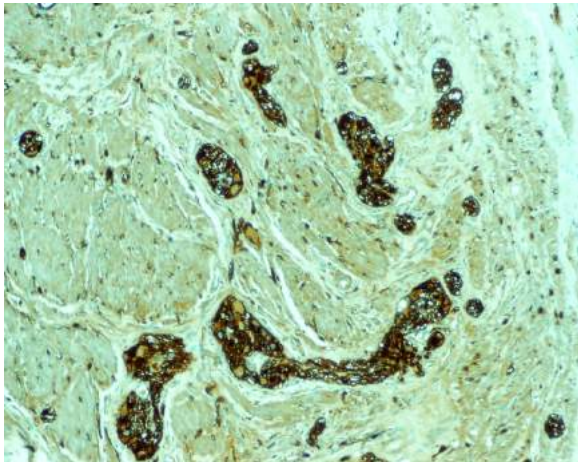


**Figure (3):** Scattered islands of neuronal tissue positive for (S-100) extending in between smooth muscle (Immunostaining x 200)

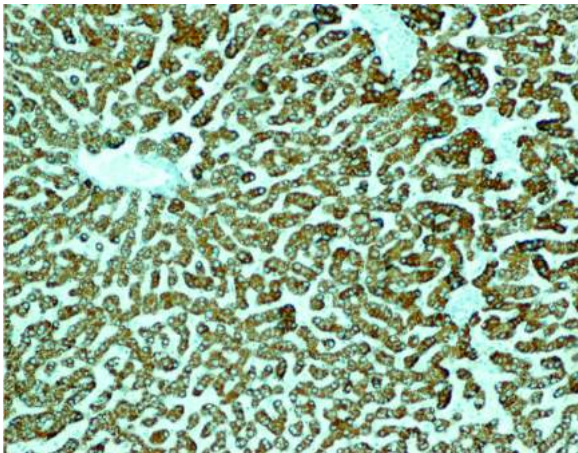


**Figure (4):** Immunohistochemical staining for Hepatocytes Specific Antigen (HSA) was strongly positive for the hepatic tissue (IHC x 200)

## DISCUSSION

Respiratory obstruction in a neonate is not uncommon. However, upper airway obstruction presenting at birth due to oropharyngeal mixed choristoma is extremely rare.

MRI and video-fluoroscopy study can be useful in the evaluation of mass lesion in oral cavity as in our case; however confirmatory diagnosis rests on microscopic examination of the tissues.

The diagnosis of mixed choristoma was based on histopathological examination and immunostaining investigations of surgically resected specimen which revealed presence of gastric, intestinal, hepatic, and neuronal tissues.

In general, choristomas are usually asymptomatic. Their clinical presentation depends on their locations. 30% of oral choristomas can present with increased salivation, altered speech, difficulty in swallowing, feeding and respiration (5,6). Those found in oropharynx and larynx can present with airway obstruction and dysphagia as seen in the present case (4). Rarely, bleeding from oral cavity can be a presenting symptom in cases of gastric choristoma due to peptic ulceration (10). Differential diagnosis of oropharyngeal choristoma should include teratoma, glioma, cystic hygroma, dermoid, hemangioma, neurofibroma, myofibroma, encephalocele (4,5,6).

Choristoma is found to be associated with other congenital anomalies such as cleft palate with tongue mass containing gastrointestinal mucosa and pancreas (7). Furthermore gastric choristoma had also been described in tongue associated with macrostomia, prognathic mandible and cleft palate (8). Its association with CHDAOM has not been reported previously. (7)

Prognosis in such cases is excellent as surgical excision is curative. Recurrences are quite common due to incomplete resection.

The aetiopathogenesis of choristoma remains obscure but several theories have been proposed to explain this. Choristoma develops from failure in the normal course of embryonic development of the neural tube which may give rise to a great variety of defects as the head and neck region develops (11).

## CONCLUSION

The choristoma is a type of developmental malformations that occur in head and neck area. Mixed choristoma presenting with upper airway obstruction at birth is extremely rare. Its association with CHDAOM is reported here for the first time. Early detection of such cases and appropriate management is warranted. Surgical excision in neonatal period allows early introduction of oral feeding, normal development of swallowing and pharyngeal coordination. Recurrence is quite common with incomplete resection.

## REFERENCES

1. Vibhuti D A, Smita SS, Hrishita VK, Madhuri SK. Cartilaginous choristoma of palatine tonsil- rare entity. National Journal of Laboratory Medicine 2014;32:16-17
2. Bernig T, Weigel S, Mukodzi S, Beck JF, Wiersbitzky H, Von Suchodoletz H et al. Ectopic thymus in 12 years old boy: a case report. *Pediatr Hematol Oncol*, 2000; 17(18):713-17
3. Haemel A, Gnepp DR, Carlsten J, Robinson-Bostom L. Heterotopic salivary gland tissue in the neck. *J Am Acad Dermatol*. 2008;58(2):251-256
4. Desuter G, Plouin-Gaudon I, de Toeuf C, Gosseye S, Hamoir M. Gastric choristoma of the midline neck in a newborn. A case report and review of the literature. *J Pediatr Surg* 2003;38:E1-3
5. Fan SQ, Ou YM, Liang QC. Glial choristoma of the tongue: Report of a case and review of the literature. *Pediatr Surg Int*, 2008; 24:515-9.
6. Said-Al-Naif N, Fantasia JE, Sciubba JJ, Ruggiero S, Sach S. Heterotopic oral gastrointestinal cyst; report of 2 cases and review of literature. *Oral Surg Oral Med Oral Pathol Oral Radiol Endod* 1999;88:80-6
7. Khunamornpong S, Yousukh A, Tananuvat R. Heterotopic gastrointestinal and pancreatic tissue of the tongue. A case report. *Oral Surg Oral Med Oral Pathol, Oral Radiol Endod* 1996;81:576-9
8. Erdem E, Tuz HH, Gunhan O. Gastric mucosal choristoma of the tongue and floor of the mouth. *J Oral Maxillofac Surg* 2001;59:210-2
9. Lin DS, Huang FY, Lin SP, et al. Frequency of associated anomalies in congenital hypoplasia of depressor angularis oris muscle: a study of 50 patients. *Am J Med Genet* 1997; 71: 215-8.
10. Srinivas T, Shetty KP, Srinivas H. Mixed heterotopic gastrointestinal cyst and extra nasal glial tissue of oral cavity with cleft palate. *Afr J Paediatr Surg* 2011;8:237040
11. Ranmeet B. Lingual cyst with respiratory epithelium: An entity of debatable histogenesis. *Journal of Oral and Maxillofacial Surgery, Medicine, and Pathology* 2012; 24(2):110–114.